Geomechanics and Engineering, *Vol. 30, No. 5 (2022) 479-487*
https://doi.org/10.12989/gae.2022.30.5.479

Field study of the process of densification of loose and liquefiable coastal soils using gravel impact compaction piers (GICPs)

Bahman Niroumand[1a] and Hamed Niroumand*[2]

[1]*Department of Civil Engineering, Faculty of Engineering, Persian Gulf University, Bushehr, Iran*
[2]*Department of Civil Engineering, Faculty of Engineering, Buein Zahra Technical University, Qazvin, Iran*

(*Received June 5, 2021, Revised May 13, 2022, Accepted August 17, 2022*)

Abstract. This study evaluates the performance of gravel impact compaction piers system (GICPs) in strengthening retrofitting a very loose silty sand layer with a very high liquefaction risk with a thickness of 3.5 meters in a multilayer coastal soil located in Bushehr, Iran. The liquefiable sandy soil layer was located on clay layers with moderate to very stiff relative consistency. Implementation of gravel impact compaction piers is a new generation of aggregate piers. After technical and economic evaluation of the site plan, out of 3 experimental distances of 1.8, 2 and 2.2 meters between compaction piers, the distance of 2.2 meters was selected as a winning option and the northern ring of the site was implemented with 1250 gravel impact compaction piers. Based on the results of the standard penetration test in the matrix soil around the piers showed that the amount of $(N_1)_{60}$ in compacted soils was in the range of 20-27 and on average 14 times the amount of (1-3) in the initial soil. Also, the relative density of the initial soil was increased from 25% to 63% after soil improvement. Also the safety factor of the improved soil is 1.5-1.7 times the minimum required according to the two risk levels in the design.

Keywords: gravel impact compaction piers; liquefaction; multilayer soil; soil compaction; soil improvement

1. Introduction

Basically, in the construction of new residential and industrial towns consisting of short buildings, industrial sheds and road network in coastal areas with the risk of liquefaction and the problem of lack of the safe bearing capacity of the soil due to high settlement, selection of soil improvement methods with high technical efficiency, low cost and high execution speed are very important. In coastal areas consisting of a multi-layered soil system with a loose top layer, the use of soil improvement methods based on natural materials due to the presence of invasive ions in coastal environments and no need for very heavy special soil improvement machines are important in choosing the method of soil improvement. Shields *et al*. (2004) proposed a method of making rammed aggregate piers (RAP) in sandy soils. In granular soils, a casing pipe is often used to maintain the stability of the cavity wall during construction. This method cannot be a desirable option, due to excavation and removing of soil from inside the casing pipe, a high volume of gravel consumed during ramming, water and silty sand rising from the bottom of the casing pipe while removing the casing pipe, the ineffectiveness of compaction the contaminated gravel mass, and the increase of cost and runtime. Vibro stone columns are one of the common options in soil improvement. However, after the implementation of stone columns, the relative density of loose soil around the columns does not change much and the load capacity of the composite soil layer is low. In addition, according to US and Indian standards, the use of stone columns is not appropriate in situations where it is not possible to place the ends of the columns on a firm bottom layer. Gravel compaction piers are similar to sandy piers with drainage performance at the time of the earthquake, with shortening of the drainage path and prevention of overpressure reduces the potential for liquefaction. Also, these piers can reduce the potential for soil liquefaction by compaction of the matrix soil, or eliminating it in general. Hatanaka *et al*. (2008) performed experiments in situ and laboratory before and after soil improvement, in order to directly evaluate and validate the effects of soil improvement by sand compaction piers on density, deformation, static strength characteristics, and sand soil liquefaction, it was concluded that the compaction sand piers increased the N number of standard penetration tests in the range of 5 to 20 and the dry density and relative density of sandy soil increased dramatically. Also with increasing density, the drained shear strength of sandy soil increased. The increase in the internal friction angle was between 3 to 5 degrees. As the relative density increased, the liquefaction resistance after sand densification had suddenly increased more than 3 times before that. Various researchers, including Aghili *et al*. (2021), Lajevardi and Enami (2021), Zhou *et al*. (2021), Yu *et al*. (2020), Shamsi *et al*. (2019), Lima *et al*. (2019), Okamura *et al*. (2006), Deb and Majee (2014), Harada and Ohbayashi (2017), Salem *et al*. (2017), Yoshimi *et al*. (1989), Okamura *et al*. (2003), Hatanaka (2008), Yu *et al*. (2020) and Farias *et al*. (2005), Sharma and Gupta (2021), Doan and Fatahi (2021), and Dar and Shah (2021) have evaluated the performance

*Corresponding author, Assistant Professor
E-mail: niroumand.mrud@gmail.com
[a]Ph.D.

ISSN: 2005-307X (Print), 2092-6219 (Online)

Table 1 Soil classification results

Depth (m)	D30 (mm)	D50 (mm)	D60 (mm)	F (%)	LL (%)	PI (%)	UCS
0.00-3.50	0.04-0.08	0.09-0.14	0.10-0.18	14-33	-	-	SM

Table 2 Particle wighted distribution

Clay (%)	Silt (%)	Sand (%)	Cravel (%)
3-7	14-27	67-86	-

Table 3 Physical and mechanical properties of natural soil

Depth (m)	ω (%)	γ_{sat} (kN/m^3)	γ_d (kN/m^3)	G_S (-)	e (-)	φ' (deg.)	C'' (kPa)
0.00-3.50	32-33	18.48	14	2.67	0.87	27-28	0.01-0.02

Table 4 Relative density results

Very Loose and Very Dense Soil				Natural Soil		Dr
e_{min} (-)	$\gamma_{d\text{-}max}$ (kN/m^3)	e_{max} (-)	$\gamma_{d\text{-}min}$ (kN/m^3)	e (-)	γ_d (kN/m^3)	(%)
0/6	16.5	0.96	13.5	0.87	14	25

Table 5 Comparison of physical properties between natural and remoulded soils

Soil Type	ω (%)	γ_d (kN/m^3)	γ_{sat} (kN/m^3)	e (-)
Natural	32	14	18.48	0.87
Remoulded	31	14	18.34	0.83

Table 6 Standard prenetration test results

Depth (m)	N	N_{60}	$(N_1)_{60}$	Dr (%)	φ' (deg.)	γ_d (kN/m^3)
0.00-3.50	1-2	1-2	2-3	18-22	26-28	14

and mechanism of stone columns as well as sand compaction piles to reduce the risk of liquefaction and improvement of soils prone to liquefaction. In 2013, the project of Persian Gulf Science and Technology Park on a coastal site consisting of a multi-layered soil system with a very loose layer of silty sand, despite various operational constraints, led to the development of a new process and technology in soil improvement. Weak and liquefiable soils became the so-called “gravel impact compaction piers” and the patent of the US.

Based on this, the new method and technology under the title of gravel impact compaction piers, which is the result of invention, was evaluated in this study.

2. Research method

2.1 Site introduction and identification of the soil

The case study was conducted in the Persian Gulf Science and Technology Park located in Bushehr port in Iran. On a 2.8-hectare coastal site, an extensive engineering embankment with a thickness of 1.8 meters has been constructed. This case study focuses specifically on the operation of improving the sandy soil bed located below the northern ring of the U-shaped complex, about 350 meters long and 15 meters wide. All laboratory and field experiments were performed according to different ASTM standards. The results of drilled boreholes indicate that the studied site was mainly implemented up to a depth of 38 meters from the top of embankment, consisting of a layer of SM with a very loose relative density (brown silty sand) with an average thickness of 3.5 m on a multi-layered system of CL with medium to hard relative consistency (brown and gray clay with low plastic property). In the study area, the technical specifications of the silty sand layer with an average thickness of 3.5 m are presented as a liquefiable layer in the form of tables 1 to 6. Table 1 shows the range of values of the parameters D30, D50 and D60, and Table 2 shows the range of values of the percentage of the constituent elements obtained from the grading curves at different depths of the sandy layer.

The range of variations in the values of physical properties of sandy soil including moisture content (ω), saturation density (γ_{sat}), dry density (γ_d), void ratio (e) and soil mechanical properties including effective internal friction angle (Φ') and effective adhesion (c') of soil are presented in Table 3. Direct shear test (DST) was used to determine soil mechanical parameters. During direct shear tests, the specimens were remoulded with great accuracy.

Table 4 shows the results of calculating the relative density of the sandy soil layer on average.

Table 5 comparatively shows the measured laboratory results showing moisture content, dry density, saturation density and void ratio for both natural and remolded soils.

Table 6 shows the initial and modified results of the standard penetration test (SPT) at different boreholes and within the sandy layer, together with the various parameters calculated based on the correlation formulas on the SPT test results. As can be seen, the results of the dry density and soil-based internal friction angle on the laboratory tests and the SPT test are relatively well adapted.

2.2 Technology and the process for construction of gravel impact compaction piers

In this method, to create a hole or cavity in the bed, instead of using a mechanical auger, a water jet or compressed air and transporting the excavated soil, the shuttle system (a casing pipe and middle shaft with closed and conical end) that can be opened and closed inside the casing pipe was used, which is hammered into the bed by a special tamper device attached to a hydraulic hammer mounted on a hydraulic excavator. Thus, the soil removal and transport item is removed and the matrix soil around the pier is compacted radially. The implementation of these piers is in three general stages includes; (first step) hammering the shuttle 1-2 times into the weak soil layer, opening and removing the middle axis and pouring gravel materials into the pipe and then removing the pipe and repeating this step if it was necessary, (second step) frequent hammering of the long penetration tamper and feeding of gravel to the bottom of the pier and (third step) implementation of an extensive gravel layer on the ground and hammering the gravel layer on the piers and matrix soils with a flat tamper device.

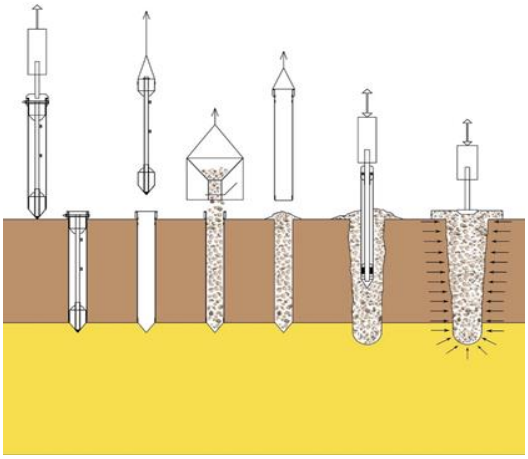

Fig. 1 Step-by-step construction of gravel impact compact piers in loose and liquefied soils

Table 7 Coarse aggregate dassification results

D10 (mm)	D30 (mm)	D50 (mm)	D60 (mm)	C_C	C_U	LL (%)	PI (%)	UCS
8-13	16-18	21-24	24-28	0.8-1.2	2.2-2.8	-	-	GP

Also, for the compaction of gravel materials inside the pier, a special tamper device with a closed and conical end connected to the hydraulic hammer mounted on the excavator is used. The diameter and length of the tamper device is less than the nominal diameter and pier length, respectively. The hammering operation is performed after filling the pier, applying a wide layer and the aggregate depot on the pier and repeatedly until the desired density is reached. The implementation steps of gravel impact compaction piers from the weak soil layer are presented in both schematic and operational forms in Fig. 1.

2.3 Components of gravel impact compaction piers

Selecting the type of material for the creation of compaction piers was according to various criteria including; (a) rapid drainage capability, (b) durability against physical disintegration due to continuous wetting and drying in the vicinity of seawater, (c) high hardness against dynamic impacts of tamper devices, (d) high density and internal friction angle, (e) having coarse-grained texture to minimize the force required to remove the shuttle and tamper device from inside the gravel cavity. However, the use of broken gravel aggregates from the calcareous rocks used in concrete placing with a diameter of 12 to 38 mm and the GP name was a good choice in terms of performance. The dry density of gravel material in dense mode and internal friction angle obtained from the direct shear test with 30×30 cm box were in the range of 14-14.5 kN/m3 and 39-41 degree, respectively. The average gravel material drop in the Los Angeles and Micro-Deval experiments were in the range of 12-18% (less than the maximum allowable drop of 35%) and 10-16% (less than the maximum allowable drop of 30%), respectively. The results of the granulation, hydrometer, and Atterberg limits tests and the percentages of the constituent elements of the gravel materials are presented in Tables 7 and 8.

Table 8 Coarse aggregate wighted distribution

Clay (%)	Silt (%)	Sand (%)	Gravel (%)
-	0.1-1	3-6	94-95

2.4 Characteristics and process of constructing gravel impact compaction piers in the test area

2.4.1 Design specifications for gravel impact compaction piers

Basically, by applying gravel impact compaction piers, retrofitting of loose sandy layer against liquefaction can be accomplished without considering four effective factors in this field, including; (a) replacement of 10 to 40% of the soil surface of the liquefiable layer with hard, non-liquefied grain materials; (b) reducing the amount of shear stresses of the soil block between the columns, (c) creating drainage columns to rapidly reduce excess pore-water pressure during the earthquake, and (d) absorbing a greater percentage of the shear stresses created in the soil layer during the earthquake, which is done only by the radial compaction of the matrix soil ("Recommendation for the Design, Calculation, Construction and Quality Control of Stone Columns under Buildings and Sensitive Structures", 2011).

Since the performance of gravel impact compaction piers are similar to gravel and sand compaction piles, therefore, the design of gravel impact compaction piers can be largely based on the principles of design of sand and gravel compaction piles. For the design of gravel and sand compaction piles four methods as A, B, C, and D are used, depending on the geotechnical characteristics of the soil layers. Methods B and C assume that no soil uplift occurs during the installation of sand compact piles. The design method used in this article is somewhat similar to method B. According to method B, after estimating the void ratios of original soil (ei) and improved soil (et) using standard penetration test results and the target (expected level after soil improvement) for matrix soil and estimation or measurement of emax and emin void ratios of original soil, the replacement area ratio is calculated from Eq. (1).

$$R_a=(e_i-e_t)/(1+e_t) \quad (1)$$

The diameter of the piles determines by calculating Ra and selecting the distance between the compaction sand piles in one of the triangular or square patterns.

Based on the design method used in this paper, if the arrangement of the gravel impact compaction piers is an equilateral triangle with a side length of S and the pier diameter (dp) determination is carried out through a single unit cell with a diameter of De (Fig. 2), in this case, assuming the cylinder boundary and unit cell height (H) remain constant, the volume of soil equivalent to the pier is injected into the volume of the cylindrical soil around the pier (matrix soil).

By equating the dry weight (W_{dry1}) of the primary unit cell soil before pier installation with dry weight (W_{dry2}) of the peripheral soil around the pier (matrix soil) in the

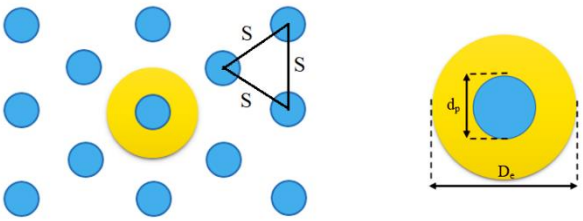

Fig. 2 Triangular arrangement and unit cell model

Table 9 Calculated unit cell parameters

S (m)	d_p (m)	D_e=1.05S (m)	R_a=0.907(dp/S)^2 (%)
1.80	0.60	1.89	10.08
2.00	0.60	2.1	8.16
2.20	0.60	2.31	6.75

R_a: replacement area

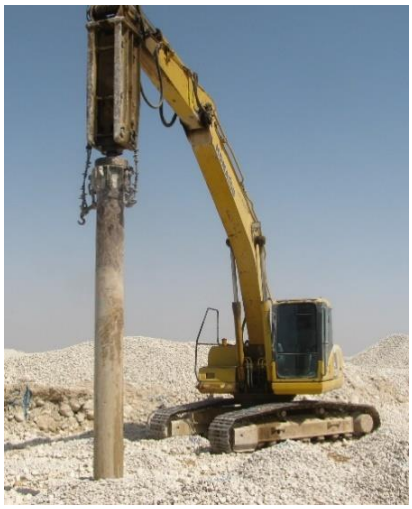

Fig. 3 Hammering the shuttle into the soil through the shuttle hammer mounted on the hydraulic hammer

secondary mode after pier installation, Eq. (2) was obtained

$$\gamma_{d_2} = \left(\frac{D_e^2}{D_e^2 - d_p^2}\right)\gamma_{d_1} \quad (2)$$

Where γ_{d1} and γ_{d2} are the primary and secondary soil dry density, respectively. Accordingly, by precisely measuring the primary dry density of the soil, selecting the distance of (S) between the compaction piers, and selecting the secondary dry density (target) of the soil matrix, the initial diameter (nominal diameter) of the compaction piers can be calculated. To select the dry density of the secondary soil (after soil improvement), after selecting the (N1)60 target, the relative density value is estimated using the correlation relationships between (N1)60 and Dr. Then, by estimating the Dr value and measuring the values of the emax and emin void ratios, the amount of improved soil void ratio (e) is obtained. Finally, using the specific gravity values (G_s), water specific gravity (γ_w) and the void ratio of the improved soil (e), the amount of specific gravity (γ_{d2}) of the improved soil is calculated.

In fact, at this stage, different combinations of S and dp are selected and after performing the required liquefaction analysis using different methods, the best option is selected technically and economically. In this study, in order to select a desirable technical option, assuming the nominal diameter of the compaction piers as a constant value, 3 different combinations were considered by changing the S parameter.

Table 9 shows the results of the calculated unit cell parameters based on the selected compaction piers option (to be sure, using nominal diameter dp rather than extended diameter). Table 10 also presents the measured and calculated (predicted) relative compaction of sandy soils based on the 3 selected options. As can be seen, it is expected that based on the radial compaction of the matrix soil, the sandy soil layer will be retrofitted with a high degree of reliability against liquefaction. In fact, reducing the S distance from 2.20 to 1.8 meters is expected to increase the $(N_1)_{60}$ value of standard penetration tests from 20 to 36. However, if the value of $(N_1)_{60}$ is obtained in practice equal to 20, the sandy layer is resistant to liquefaction as needed.

2.4.2 Construction technology of gravel impact compaction piers

According to the invention USPATENT 9915051B2 and per Fig. 1, for the construction of gravel impact compaction piers in weak soil layer, three categories of technical equipment have been prepared including; (a) casing pipe installation equipment including a shuttle with conical end, (b) devices to pour gravel into the casing pipe containing conical hopper, and (c) The gravel compaction devices inside the cavity, including the long and flat tamper devices. The shuttle hammering into the soil was carried out by a hydraulic excavator equipped with a hydraulic hammer and a shuttle mounted on the hammer (Fig. 3). As a result of this process, carrot-shaped compaction piers with a length of more than 3.5 m, an end diameter of about 60 cm, a top diameter of about 85-90 cm and an average diameter of 75 cm were created. During this operation, various hydraulic hammers with a weight in the range of 1.2-1.5 tons with 400-650 beats per minute were used.

Fig. 4 shows the location and executive priority of the gravel impact compaction piers in each of the selected

Table 10 Comparison of relative density before and after improvement

time	e (-)	γ_d (kN/m^3)	ω (%)	γ_{sat} (kN/m^3)	Dr (%)	$(N_1)_{60}$
before Improvement (measured)	0.87	14	32	18.48	25	2-3
after Improvement (calculated for S=1.80 m)	0.68	15.57	25	19.46	78	36
after Improvement (calculated for S=2.00 m)	0.762	15.24	27	19.35	67	27
after Improvement (calculated for S=2.20 m)	0.75	15	28	19.20	58	20

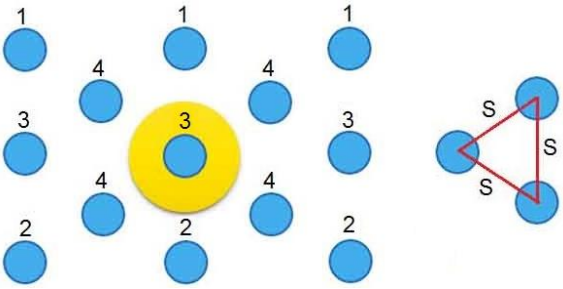

Fig. 4 Display the sequence and priority of the gravel impact compaction piers in each of the 3 selected options

options in the pilot phase. In this study, in order to technically evaluate the design, 3 options with a triangular pattern, under the nominal diameter of the compaction piers were considered constant and equal to 60 cm and distances of 1.8, 2 and 2.2 m. For each option, 13 compaction piers were built and the ground was completely improved to a 6 x 8.5 piece. In total, 3 plots of land with an area of 51 square meters each, in the vicinity of each other in the pilot phase, were improved and performed the necessary experiments using gravel impact compaction piers.

3. Results

At the time of the pilot, the groundwater level due to seawater was about 0.5 meters below the normal ground level. However, during the implementation of the improvement plan using gravel impact compaction piers even in sea condition and the presence of 0.5 m of water on the site, the compaction piers were implemented. Immediately after the implementation of each of the piers, the soil matrix around the piers became liquefied and unstable due to the immediate increase of the pore water pressure and the decrease of the effective soil stress caused by the dynamic shuttle impact. Subsequently, with the full implementation of the piers, the desired soil range became extremely unstable. The instability was such that it was not possible to move the hydraulic excavator, and with the impact of the excavator cup on the surface of the bed, a wave-like movement of the soil layer was observed. Due to the immersion of the desired area, the outflow and discharge of water through gravel piers was well observed. Daily surveys showed that after 11-14 days, the sandy soil layer was stable and resistant. So that it was possible to move the chain hydraulic excavator easily on it. With the completion of the next steps, including the application of an extensive layer of gravel and ballast with a thickness of about 40 cm on the desired area and implementation of a long tamper, after about 7-10 days, the sandy layer reached a higher level of stability and resistance. In the pilot phase, the relative density control of the soil block around the compaction piers was performed through standard penetration testing. In addition, boreholes were drilled in the matrix soil, and intact specimens were tested for density and moisture content. The location of standard penetration and sampling tests for each of the experimental options is shown in Fig. 5.

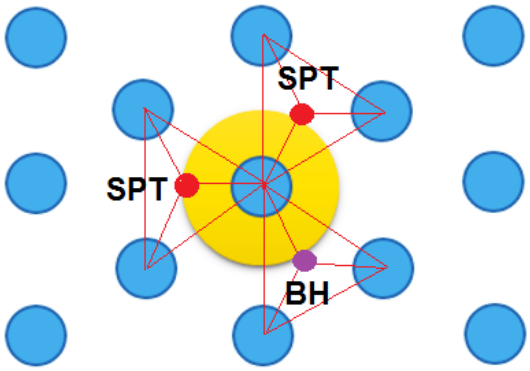

Fig. 5 Schematic details of standard penetration tests (SPT) and well boring (BH) for each selected option

Table 11 SPT results on the matrix soils after improvement

Depth (m)	S=1.80 m			S=2.00 m			S=2.20 m		
	N_{SPT1}	N_{SPT2}	$N_{avg(S=1.80m)}$	N_{SPT3}	N_{SPT4}	$N_{avg(S=2.00m)}$	N_{SPT5}	N_{SPT6}	$N_{avg(S=2.20m)}$
0.5	33	35	34	26	28	3\27	21	22	22
1	33	34	34	25	26	26	20	21	21
1.5	31	32	32	25	25	25	19	20	20
2	28	29	29	23	24	24	18	20	19
2.5	26	26	26	22	22	22	18	19	19
3	23	24	24	19	20	20	16	16	16

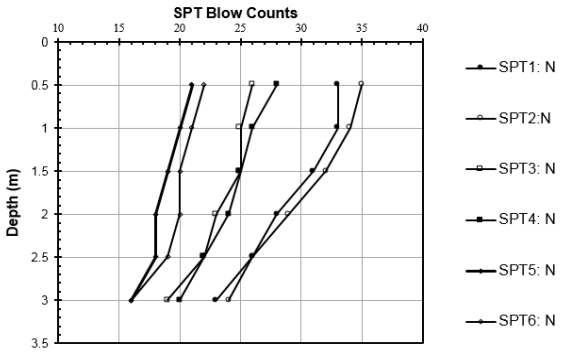

Fig. 6 Comparison of N-values variation curves of standard penetration tests after soil improvement for three test areas including: (a) SPT1 and SPT2 for S=1.80 m, (b) SPT3 and SPT4 for S=2.0 m, and (c) SPT5 and SPT6 for S=2.20 m

3.1 Standard penetration test results

In this study, the layering and technical properties of the sandy soil in the study area and under the improvement operation which was done by gravel impact compaction piers had a relatively good uniformity. In this regard, to investigate the relative density of the improved soil in the experimental areas, 2 standard penetration tests were carried out up to a depth of 3.5 m at 0.5 m intervals and sampling by drilling a borehole to a depth of 3.5 m for Each of the 3 experimental areas. Table 11 shows the results of 6 standard penetration tests in designated locations after completion of soil improvement operations for 3 experimental areas. As can be seen, for each experimental area, with increasing depth, the N value of the SPT test has a downward trend. In fact, due to the carrot shape of compaction piers and the decrease in pier diameters, with depth increasing, the

Table 12 Comparison of SPT results on the matrix soils before and after improvement

Depth	before soil improvement			after soil improvement S=1.80 m			after soil improvement S=2.00 m			after soil improvement S=2.20 m		
	N	N_{60}	$(N_1)_{60}$	$N_{avg(1-2)}$	$N_{60\text{-}avg}$	$(N_1)_{60\text{-}avg}$	$N_{avg(3-4)}$	$N_{60\text{-}avg}$	$(N_1)_{60\text{-}avg}$	$N_{avg(5-6)}$	$N_{60\text{-}avg}$	$(N_1)_{60\text{-}avg}$
0.5	2	2	3	34	26	44	26	20	34	22	16	27
1	1	1	1	34	26	44	25	19	32	21	16	27
1.5	2	2	3	32	24	41	25	19	32	20	15	26
2	1	1	1	29	22	37	23	17	29	19	15	24
2.5	2	2	3	26	20	34	22	16	27	19	14	24
3	2	2	2	24	18	31	19	14	24	16	12	20

Table 13 Calculation of safety factor against liquefaction by different methods at a_{max}=0.3 and M=6.75 before soil improvement

Depth (m)	Safety Facor Based on M=6.75 & a_{max}=0.30								Average safety Factor
	NCEER Workshop (1997)	Boulanger and Idriss (2004)	Vancouver Task Force (2007)	Chinese Code	Seed *et al.* (1983)	Tokimatsu and Yoshimi (1983)	Shibata (1981)	Kokusho *et al.* (1983)	
0.5	0.18	0.32	0.18	0.25	0.48	0.47	0.66	0.52	0.38
1	0.16	0.29	0.16	0.24	0.47	0.44	0.66	0.5	0.37
1.5	0.18	0.32	0.18	0.26	0.49	0.48	0.67	0.52	0.39
2	0.16	0.29	0.16	0.25	0.48	0.45	0.67	0.5	0.37
2.5	0.19	0.32	0.19	0.26	0.49	0.49	0.68	0.53	0.39
3	0.19	0.33	0.19	0.27	0.5	0.49	0.68	0.53	0.40

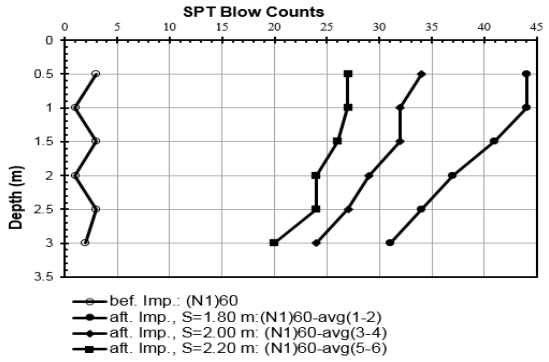

Fig. 7 Comparison of variation curves of changes in average values of $(N_1)_{60}$ in Standard penetration experiments in terms of depth, before and after soil improvement for three experimental areas including: (a) S=1.80 m, (b) S=2.0 m, and (c) S=2.20 m

maximum N-value occurs at the top and the minimum N-value at the end of the pier. Fig. 6 shows the comparison of the N-values variation curves of the standard penetration tests performed in 3 experimental areas of the site after soil improvement. As can be seen, as the distance between the compaction piers in the triangular pattern decreases, the radial density of the soil increases.

Table 12 shows the average values of standard penetration tests includes N, N60 and $(N_1)_{60}$ comparatively, before and after soil improvement for 3 experimental areas. Also in Fig. 7 variation curves of $(N_1)_{60}$ in standard penetration tests before and after soil improvement are presented comparatively. Based on the results shown in Table 12, the changes of $(N_1)_{60}$ before soil improvement are in the range of 1-3 and after soil improvement, for 3 experimental areas with distances of 1.8, 2 and 2.2 meters are 31-44, 24-34 and 20-27, respectively. Also, in the depth range of the sandy soil layer, the amount of $(N_1)_{60}$ in compacted soils with distances of 1.8, 2 and 2.2 m was equal to 19, 14 and 12 times as much as in the primary soil (before improvement).

3.2 Results of liquefaction analysis

In principle, various analytical and numerical methods have been developed to analyze the liquefaction of improved soils using methods based on aggregate piers. As a popular method, Priebe (1995, 1998) presented a method of calculating the safety factor against liquefaction for vibro stone columns based on gravel column drainage characteristics, structural modification of soil texture and thereby increasing soil shear strength and the matrix soil density. In practice, the hassle of making a valid prediction is easily resolved by specifying the corrected amount of soil dry density through speculation. Based on the experience gained from the application of gravel impact compaction piers, it is possible to retrofit the liquefiable layer solely by optimally increasing the radial compaction of the matrix soil. The results of the initial soil liquefaction analysis (before improvement) at the L1 risk level (M=6.75, a_{max}= 0.3, FS_{min}=1.5) for a 75-year return period is shown in Table 13 and at the L2 risk level (M=6.75, a_{max}=0.3, FS_{min}=1) for a 475-year return period is shown in Table 14. Accordingly, the values of the safety factor against liquefaction using 8 common methods for L1 risk level are in the range of 0.37-0.40 (less than 1.5) and in the risk level of L2 it is in the range of 0.28- 0.30 (Less than 1).

As the same way, the results of liquefaction analysis on improved soil based on the third option (S=2.20 m) at L1 risk level (M=6.75, a_{max}=0.3, FS_{min}=1.5) for a 75-year return period are shown in Table 15 and at L2 risk level (M=6.75, a_{max}=0.3, FS_{min}=1) for a 475-year return period

Table 14 Calculation of safety factor against liquefaction by different methods at a_{max}=0.3 and M=7.5 before soil improvement

Depth (m)	Safety Facor Based on M=7.50 & a_{max}=0.30								Average safety Factor
	NCEER Workshop (1997)	Boulanger and Idriss (2004)	Vancouver Task Force (2007)	Chinese Code	Seed *et al.* (1983)	Tokimatsu and Yoshimi (1983)	Shibata (1981)	Kokusho *et al.* (1983)	
0.5	0.14	0.24	0.14	0.19	0.37	0.36	0.5	0.39	0.29
1	0.12	0.22	0.12	0.18	0.36	0.34	0.51	0.38	0.28
1.5	0.14	0.24	0.14	0.19	0.37	0.36	0.51	0.4	0.29
2	0.12	0.22	0.12	0.19	0.36	0.34	0.51	0.39	0.28
2.5	0.14	0.25	0.14	0.2	0.37	0.37	0.51	0.4	0.30
3	0.14	0.25	0.14	0.2	0.38	0.37	0.52	0.4	0.30

Table 15 Calculation of safety factor against liquefaction by different methods at a_{max}=0.3 and M=6.75 before soil improvement

Depth (m)	Safety Facor Based on M=6.75 & a_{max}=0.30								Average safety Factor
	NCEER Workshop (1997)	Boulanger and Idriss (2004)	Vancouver Task Force (2007)	Chinese Code	Seed *et al.* (1983)	Tokimatsu and Yoshimi (1983)	Shibata (1981)	Kokusho *et al.* (1983)	
0.5	3	3.32	3	3	2.82	3	2.93	1.86	2.87
1	2.91	2.98	2.91	2.91	2.35	2.57	2.28	1.64	2.57
1.5	2.84	2.3	2.84	2.5	2.09	2.06	1.92	1.53	2.26
2	2.81	1.86	2.81	2.06	1.9	1.74	1.67	1.45	2.04
2.5	2.8	1.55	2.8	1.78	1.74	1.53	1.49	1.38	1.88
3	2.8	1.31	2.8	1.59	1.6	1.39	1.36	1.32	1.77

Table 16 Calculation of safety factor against liquefaction by different methods at a_{max}=0.3 and M=7.50 before soil improvement

Depth (m)	Safety Facor Based on M=7.50 & a_{max}=0.30								Average safety Factor
	NCEER Workshop (1997)	Boulanger and Idriss (2004)	Vancouver Task Force (2007)	Chinese Code	Seed *et al.* (1983)	Tokimatsu and Yoshimi (1983)	Shibata (1981)	Kokusho *et al.* (1983)	
0.5	2.42	2.53	2.42	2.42	2.15	2.42	2.24	1.41	2.25
1	2.22	2.27	2.22	2.22	1.79	1.96	1.74	1.25	1.96
1.5	2.16	1.75	2.16	1.	1.59	1.56	1.46	1.16	1.72
2	2.13	1.41	2.13	1.56	1.44	1.32	1.27	1.1	1.55
2.5	2.12	1.17	2.12	1.35	1.32	1.16	1.13	1.05	1.43
3	2.12	0.99	2.12	1.2	1.21	1.05	1.03	1	1.34

Table 17 Comparison of safety factor against liquefaction between before and after improvement at two level of risk

Depth (m)	Bef. Improvement		Aft. Improvement S=1.80 m		Aft. Improvement S=2.00 m		Aft. Improvement S=2.20 m	
	$FS(L_1)$	$FS(L_2)$	$FS(L_1)$	$FS(L_2)$	$FS(L_1)$	$FS(L_2)$	$FS(L_1)$	$FS(L_2)$
0.5	0.38	0.29	3.04	2.45	2.95	2.36	2.87	2.25
1	0.37	0.28	2.97	2.25	2.83	2.15	2.57	1.96
1.5	0.39	0.29	2.88	2.19	2.76	2.09	2.26	1.72
2	0.37	0.28	2.80	2.13	2.70	2.05	2.04	1.55
2.5	0.39	0.3	2.77	2.1	2.70	2.04	1.88	1.43
3	0.4	0.3	2.74	2.06	2.27	1.71	1.77	1.34

L_1: (M=6.75, a_{max}=0.30, FS_{min}=1.5
L_2: (M=7.5, a_{max}=0.30, FS_{min}=1)

are shown in Table 16. Accordingly, the calculated safety factor against liquefaction using 8 common methods for the L1 risk level is ranged from 1.77 to 2.87 (greater than 1.5) and at the L2 risk level is in the 1.34-2.25 (more than 1).

Fig. 8 and Table 17 illustrate the values of safety factors against liquefaction comparatively for soil conditions before and after improvement at the two risk levels of L1 and L2 for 3 experimental areas, respectively. As can be seen, based merely on the effect of the radial compaction of the compaction piers on the matrix soil, the obtained safety factors are sufficiently higher than the minimum values required at each hazard level. On this basis, in order to

Table 18 Comparison of calculated and measured soil compaction parameters before and after improvement

S (m)	time	e (-)	γ_d (kN/m^3)	ω (%)	γ_{sat} (kN/m^3)	Dr (%)
-	before Improvement (measured)	0.87	14	32	18.48	25
1.80	after Improvement (calculated)	0.68	15.57	25	19.46	78
	after Improvement (measured)	0.67	15.68	25	19.60	79
2.00	after Improvement (calculated)	0.72	15.24	27	19.35	67
	after Improvement (measured)	0.71	15.31	26	19.29	69
2.20	after Improvement (calculated)	0.75	15	28	19.20	58
	after Improvement (measured)	0.73	15.13	27	19.21	63

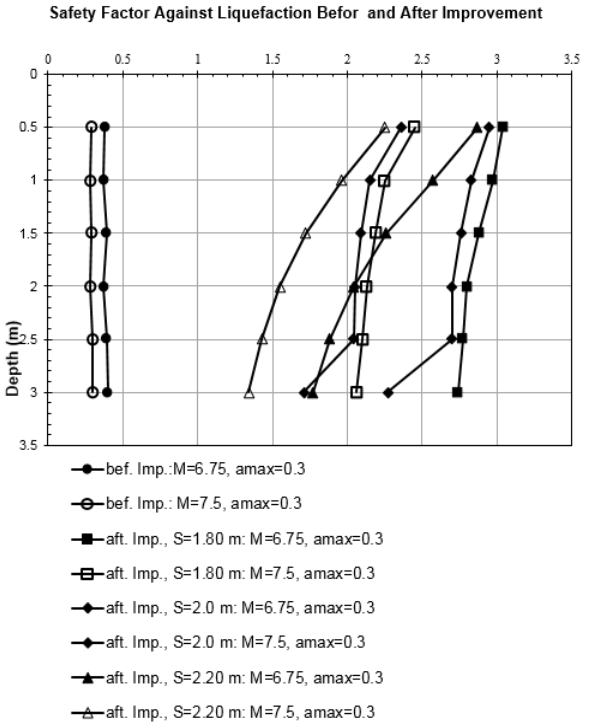

Fig. 8 Comparison of the safety factor values against liquefaction for soil conditions before and after improvement, at two risk levels of L1 and L2 for 3 experimental areas including: (a) S=1.80 m, (b) S=2.0 m, and (c) S=2.20 m

retrofitting the sand layer against liquefaction, selecting the option of gravel impact compaction piers with a triangular pattern and S=2.20 m is a technical and economical option.

3.3 Measurement of density and moisture content of soil

Despite the impossibility of obtaining undisturbed samples from saturated loose silty sand soils, in semi-deep conditions, it is possible to obtain undisturbed samples by shelby tube in case of high compaction for these types of soils. In this regard, after implementation of gravel impact compaction piers and increasing the radial compaction of the matrix soil, a shelby tube was prepared and the local moisture content and density of soil were determined. Table 18 shows a comparison between the measured and calculated results for the void ratio, dry density, moisture content, saturation density, and soil relative compaction parameters before and after soil improvement. As can be seen, for each of the experimental areas, the predicted and measured values in the after improvement conditions show a relatively good fit. However, the measured parameters have relatively higher values than the predicted parameters. In fact, by increasing the distance between the compaction piers, despite the nominal diameter of the pier being equal to 60 cm, a larger diameter is created in practice for the compaction pier.

4. Conclusions

The results of the pilot project of strengthening a very loose silty sand layer with a thickness of 3.5 m using gravel impact compaction piers in 3 experimental areas are as follows;

- Due to the implementation of an extensive gravel layer on the sandy soil layer improved by the use of gravel impact compaction piers and the application of high energy due to dynamic impact of the gravel layer surface by flat tamper device and frequent movement by the hydraulic excavator on it, it is desirable to prevent the swelling of the upper part of the matrix soil caused by the construction of the compaction pier in a desirable way. Based on this, the initial calculations for determining the required diameter for compaction piers with relatively good accuracy can be done from the idea of a unit cell assuming no swelling of the matrix soil.
- The selection of all three experimental options for the implementation of gravel impact compaction piers with a nominal diameter of 60 cm and distances of 1.8, 2 and 2.2 m was successful in order to strengthen the loose sandy layer against liquefaction. However, the use of the third option (S=2.20 m) as an economic option was given priority.
- With the implementation of gravel impact compaction piers according to the third option (S=2.20 m), on average, in the depth of sandy soil layer, the $(N1)_{60}$ amount of compacted soils in the range of 20-27 was obtained 14 times the amount of (1-3) in the primary soil.
- With the implementation of gravel impact compaction piers according to the third option (S=2.20 m), on average, without relying on the drainage property of compaction piers and without taking into account the change of the initial structure of the soil, the values of safety factor calculated against liquefaction are relied solely on the density of compaction piers, using 8 common methods for L1 risk level in the range of 1.77-

2.87 and an average of 2.23 more than the minimum required value (1.5) and in the L2 risk level in the range of 1.34-2.25 and on average 1.70 greater than the minimum required value (1).

• With the implementation of gravel impact compaction piers in accordance with the third option (S=2.20 m), on average, in the depth range of sandy soil layer, the safety factor calculated against the compacted soil liquefaction are 4.5-7.5 times the same amount in the primary soil (before improvement).

• By implementing gravel impact compaction piers, through creating repeated radial compaction for the matrix soil in the process of hammering and feeding the gravel, the first time shuttle, hammering and feeding the gravel, the second time, hammering and feeding the gravel repeatedly by the long tamper, and hammering and feeding of gravel is frequently done by a flat tamper device, with increasing pore-water pressure, the desired area is artificially liquefiable and highly unstable, and becomes stable and resistant within 11-14 days.

• With the implementation of gravel impact compaction piers according to the third option (S=2.20 m), the relative density of primary soil increased from 25% to 63% (about 2.5 times increase) and the dry density of primary soil increased from 14 to 15.13 kN/m^3 (about 8% increase). Also, with increasing soil density around the compaction piers, the percentage of soil moisture decreased on average from 32% to 27%.

• Gravel impact compaction piers are a self-regulating system for increasing relative soil density. In fact, gravel injection is done through gravel columns created under a specified energy level of the hydraulic hammer installed on the hydraulic excavator and is done as long as it is not possible to inject gravel. Based on this, it creates a uniform stiffness modulus for the subgrade.

• The soil improvement method using gravel impact compaction piers is a definitive soil improvement method and after the improvement operation, soil compaction can be measured.

Acknowledgment

We sincerely thank the board of directors and the specialized team of High-Tech Company of Asian Soil Improvement (ASI) and companies in carrying out complementary geotechnical controls and addressing technical challenges created during the various stages of technical equipment construction.

References

Aghili, E., Hosseinpour, I., Chenari, R. J., Ahmadi, H. (2021), "Behavior of granular column-improved clay under cyclic shear loading", Transportation Geotechnics. https:// doi.org/10.1016/j.trgeo.2021.100654

Barksdale, R. D. and Bachus, R. C. (1983), "Design and Construction of Stone Columns", Volume II, National Technical Information Service.

Farias, M. M. Nakai, T. Shahin, H. M. Pedroso, D. M. Passos, P. G. O. and Hinokio, M. (2005), "Ground Densification Due to Sand Compaction Piles", In Soils and Foundations. Https: //doi.org/10.3208/sandf.45.2_167.

Prieb, H. J. (1995), "The Design of Vibro Replacement", Ground Engineering. Https: //doi.org/10.1016/0148-9062 (96)80092-1.

Harada, K. and Ohbayashi, J. (2017), "Development and Improvement Effectiveness of Sand Compaction Pile Method as a Countermeasure against Liquefaction", Soils and Foundations. Https: //doi.org/10.1016/j.sandf.2017.08.025.

Hatanaka, M. Feng, L. Matsumura, N. and Yasu, H. (2008), "A Study on the Engineering Properties of Sand Improved By the Sand Compaction Pile Method", Soils and Foundations. Https: //doi.org/10.3208/sandf.48.73.

Kitazume, M. (2005), "The Sand Compaction Pile Method". https://doi.org/10.1201/9781439824696.

Lajevardi, S. H. Enami, S. (2021), "Small scale behavior of stone columns encased by tires", Geomechanics and Engineering, https://doi.org/10.12989/gae.2021.25.5.429

Lima, B. T., Almeida, MSS, Hosseinpour, I. (2019), "Field measured and simulated performance of a stone columns-strengthened soft clay deposit", International Journal of Geotechnical Engineering, https://doi.org/10.1080/19386362.2019.1653506

Niroumand, B. (2017), 9840835. United States of America. https://doi.org/E02D 3/10 (20060101); E03F 1/00 (20060101); E02D 1/00 (20060101).

Okamura, M. Ishihara, M. and Oshita, T. (2003), "Liquefaction Resistance of Sand Deposit Improved With Sand Compaction Piles", Soils and Foundations. https://doi.org/10.3208/sandf.43.5_175.

Okamura, M. Ishihara, M. and Tamura, K. (2006), "Degree of Saturation and Liquefaction Resistances of Sand Improved With Sand Compaction Pile", Journal of Geotechnical and Geoenvironmental Engineering. https://doi.org/10.1061/(ASCE)1090-0241(2006)132:2(258).

Priebe, H. J. (1998), " Vibro Replacement to Prevent Earthquake Induced Liquefaction", Ground Engineering.

(2013), "Recommendations for the Design, Calculation, Construction and Quality Control of Stone Columns under Buildings and Sensitive Structures", Revue Française de Géotechnique. https://doi.org/10.1051/geotech/2013144051.

Salem, Z. B., Frikha, W., Bouassida, M. (2017), "Effects of densification and stiffening on liquefaction risk of reinforced soil by stone columns", Journal of Geotechnical and Geoenvironmental Engineering., https://doi.org/ 10.1061/(ASCE)GT.1943

Shamsi, Y, Wang, Z, and Sun, H. Y. (2020), "Behavior of sand columns reinforced by vertical geotextile encasement and horizontal geotextile layers", Geomechanics and Engineering, https://doi.org/ 10.12989/gae.2019.19.4.329

Shields, C. S. FitzPatrick, B. T. and Wissmann, K. J. (2004), "Modulus Load Test Results for Rammed Aggregate PiersTM in Granular Soils", In Geotechnical Special Publication. https://doi.org/10.1061/40713(2004)54.

Zhou, Y. G., Liu, K., Sun, Z. B., Chen, Y. M. (2021), "Liquefaction mitigation mechanisms of stone column-improved ground by dynamic centrifuge model tests", Soil Dynamics and Earthquake Engineering, https://doi.org/10.1016/j.soildyn.2021.106946

Yoshimi, M. Ghanbari, A. and Nazariafshar, J. (2019), "Liquefaction Resistance of a Partially Saturated Sand", Soils and Foundations. https://doi.org/10.3208/sandf1972.29.3_157.

Yu, Y, Wang, Z, and Sun, H. Y. (2020), "Optimal design of stone columns reinforced soft clay foundation considering design robustness", Geomechanics and Engineering, https://doi.org/10.12989/gae.2020.22.4.305